Electronic States of Sodium Dimer in Ammonia Clusters: Theoretical Study of Photoelectron Spectra for $Na_2^-(NH_3)_n$ ($n = 0-6$)

Kenro Hashimoto,* Toshihiko Shimizu, and Kota Daigoku

Department of Chemistry, Tokyo Metropolitan University, 1-1 Minami-Ohsawa, Hachioji, Tokyo 192-0397, Japan

Received: August 12, 2006; In Final Form: December 9, 2006

The geometries, energetics, and vertical detachment energies of $Na_2^-(NH_3)_n$ ($n = 0-6$) were examined by ab initio molecular orbital methods in connection with their photoelectron spectra. One of the Na atoms is selectively solvated in the most stable structures for each n. The solvated Na is spontaneously ionized and the formation of a solvated electron occurs with increasing n, giving rise to the $Na^- - Na^+(NH_3)_n(e^-)$-type state. The ground and two lowest-lying excited states derived from the $1^1\Sigma_g^+$, $1^3\Sigma_u^+$, and $1^3\Pi_u$ states of Na_2, respectively, are of ion-pair character though the $1^3\Sigma_u^+$-type state has an intermediate nature slowly changing to the radical-pair state with increasing n. On the other hand, the higher states stemming from the $1^1\Sigma_u^+$, $1^3\Sigma_g^+$, and $1^1\Pi_u$ states of Na_2 show a developing radical-pair nature as n increases. The size dependences of the photoelectron spectra such as the near parallel shifts of the first and second bands, as well as the rapid red shifts of the higher bands, are studied on the basis of the electronic change of the neutrals by solvation.

1. Introduction

Microscopic solvation of metals is one of the fundamental research subjects in many areas of physics and chemistry. Clusters consisting of a single alkali atom or alkali-earth monocation and a finite number of polar solvent molecules are considered as models for microscopically investigating the charge transfer from a metal to a solvent, forming the solvated metal cation and solvated electron, and thus have been the targets of intensive studies.[1,2] The size dependence of their electronic levels has been examined by spectroscopic measurements such as photoionization-mass spectra,[3−9] photoelectron spectra,[7−9] and absorption spectra.[10−26] Several theoretical and simulation studies have been reported regarding the ionization of alkali atoms in solvent clusters and liquid solvents.[27−35] In addition, many quantum chemical calculations have been conducted to gain insight regarding the size and geometry dependences of the electronic state of the clusters.[36−48]

On the other hand, only a few studies on solvated metal aggregates have been reported so far, though they are indispensable for the microscopic understanding of metal−solvent interaction at the metal surface. Their spectra are expected to differ from those of the solvated single metal atom or ion, and an interesting change is found between $Na^-(NH_3)_n$[8] and $Na_2^-(NH_3)_n$[49,50] in their photoelectron spectra (PES). For the former clusters, the first intense band corresponding to the $3^2S(Na)-3^1S(Na^-)$ transition observed at 0.55 eV for Na^- is slightly shifted to the lower electron binding energy (EBE) at $n = 1$ but remains at almost the same EBE for larger $n \leq 12$, while the second weak band for the $3^2P(Na)-3^1S(Na^-)$ transition is rapidly red-shifted from 2.65 eV at $n = 0$ to ∼1.2 eV for $n = 4-12$. Similar band shifts are observed for the $3^2P(Na)-3^2S(Na)$-type transition in the absorption spectra of the neutral $Na(NH_3)_n$.[25] On the other hand, the PES of $Na_2^-(NH_3)_n$ have been examined for $n = 0-8$ using the 3.50-eV (355-nm) detachment light.[49,50] The spectra for $n = 0-6$ are shown in Figure 1a. The first band at 0.55 eV for Na_2^- is red-shifted to ∼0.4 eV at $n = 1$ and is gradually shifted back as n increases. The positions of the second band are almost unchanged for $n = 0-3$ but are gradually shifted to the higher EBE for larger n. In contrast, the third and higher bands are rapidly red-shifted with increasing n and are superimposed on the second band for $n \geq 4$.

We previously studied $M^-(NH_3)_n$ and $M^-(H_2O)_n$ (M = Na and Li) clusters and their neutrals with n up to four by ab initio molecular orbital methods.[45−48] NH_3 molecules are bound to Na^- from the N side, and the spatial expansion of Na 3s electrons occurs by the addition of solvent molecules in both the anionic and neutral states. The growing diffuse one-center ion-pair nature in the neutrals is responsible for the remarkable narrowing of 3^2P-3^2S separations, namely, the red shifts of the bands in the spectra. We have also carried out preliminary calculations for $Na_2^-(NH_3)_n$ and have suggested the assignment of the photoelectron bands for $n \leq 3$.[49] However, the electronic change of sodium dimer during solvation is not yet well understood.

In this study, we have extended the research to $n = 6$ calculating the geometries, total binding energies, and vertical detachment energies of $Na_2^-(NH_3)_n$. The electron distribution of the $Na_2^-(NH_3)_n$ anions has been examined in detail, and the nature of the ground and low-lying excited states of the neutral clusters has been investigated to unveil what electronic states are reflected in the observed spectra.

2. Methods

Molecular structures of $Na_2^-(NH_3)_n$ ($n = 0-6$) were optimized at the second-order Møller−Plesset perturbation (MP2) level with the 6-31++G(d,p) basis set with the usual frozen core approximation using Gaussian-98.[51] Harmonic frequencies were calculated to characterize the nature of stationary points. If an optimized structure had one or more imaginary frequencies,

* To whom correspondence should be addressed. Fax: +81-42-677-1352. E-mail: hashimoto-kenro@c.metro-u.ac.jp.

10.1021/jp0652188 CCC: $37.00
Published on Web 02/22/2007

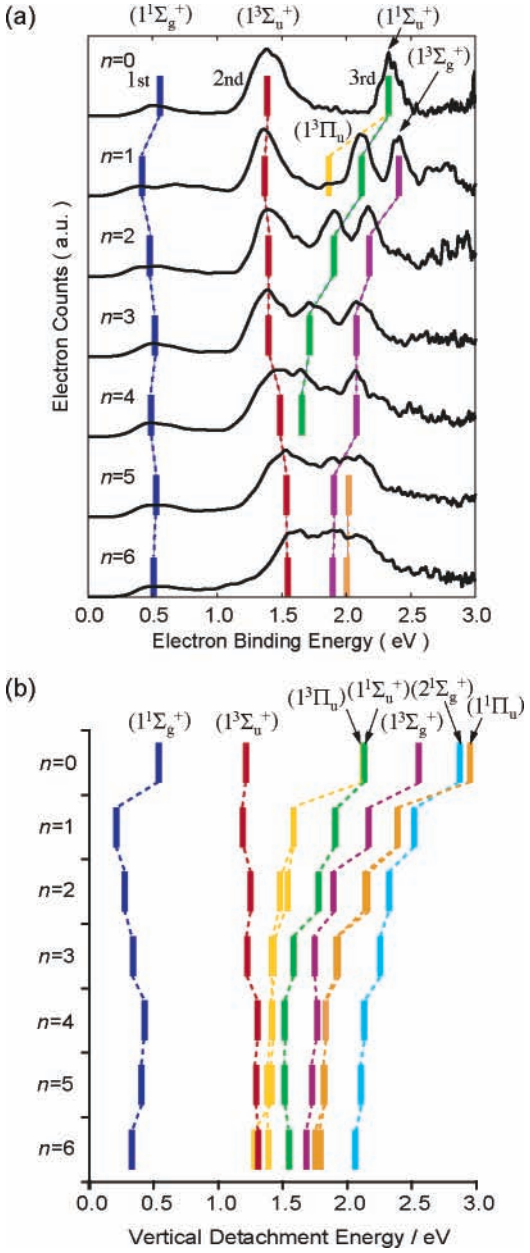

Figure 1. (a) Photoelectron spectra of $Na_2^-(NH_3)_n$ ($n = 0-6$) by the detachment energy of 3.50 eV (355 nm). Peak positions are indicated by color bars. (b) Calculated vertical detachment energies of $Na_2^-(NH_3)_n$ at the most stable structures for each $n = 0-6$.

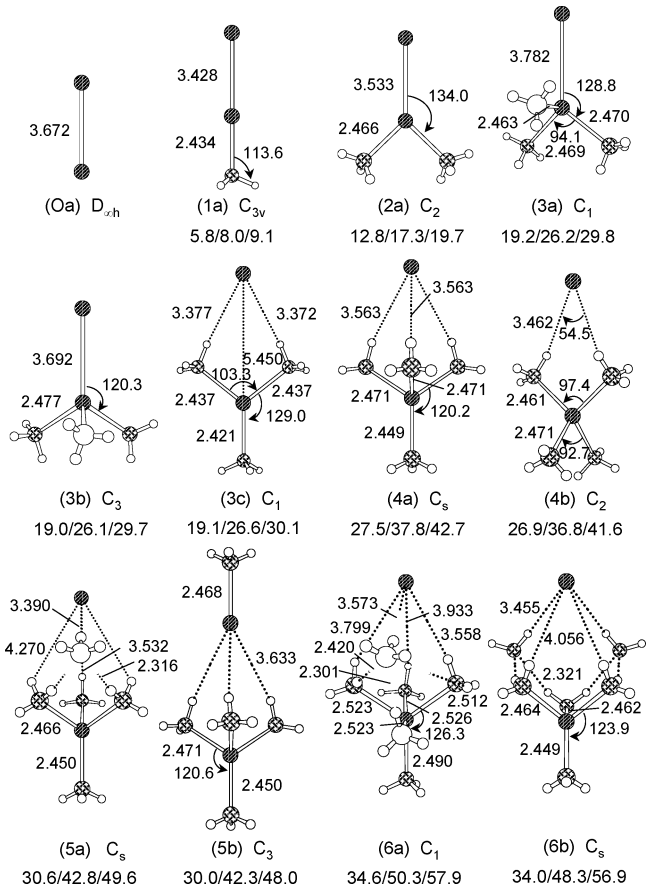

Figure 2. The most stable structures of $Na_2^-(NH_3)_n$ ($n = 0-6$) at the MP2/6-31++G(d,p) level. Geometric parameters are given in angstroms and degrees. Molecular symmetry and total binding energies (kcal/mol) with both ZP and CP corrections, with only ZP correction, and without ZP and CP corrections are given under each structure.

further optimization following the imaginary normal modes was carried out until the true local minimum was reached.

Total binding energies were calculated by the following formula:

$$-\Delta E(n) = E(Na_2^-(NH_3)_n) - E(Na_2^-) - nE(NH_3) \quad (1)$$

The zero-point (ZP) vibrational energies were evaluated using the scaled harmonic frequencies. The scale factor (0.932) was determined from the average ratio of the experimental fundamental[52] and calculated harmonic frequencies for an isolated NH_3 molecule. The basis set superposition error (BSSE) was assessed by the counterpoise (CP) method.[53] The relaxation energy term[54] was taken into account in the CP correction.

The vertical detachment energies (VDEs) of the transitions from the anionic state to the ground and low-lying excited states of the neutral $Na_2(NH_3)_n$ were calculated by the multireference single and double excitation configuration interaction (MRSDCI) method preceded by the complete active space self-consistent-field (CASSCF) calculations[55-59] using MOLPRO-2002.[60] The active space for the CASSCF consisted of 10 molecular orbitals (MOs) corresponding to the $4\sigma_g$, $4\sigma_u$, $2\pi_u$, $5\sigma_g$, $2\pi_g$, $5\sigma_u$, $6\sigma_g$, and $6\sigma_u$ orbitals on Na_2. For the anions, the CASSCF wave function was optimized for the ground state. For the neutrals, five low-lying states were averaged with equal weight for the singlet, while four low-lying states were averaged for the triplet. The natural orbitals (NOs) obtained by the CASSCF were used as one-particle functions in the MRSDCI calculations from the CASSCF references. All single and double excitations from the active orbitals on Na_2 as well as n high-lying occupied orbitals mainly corresponding to lone pair orbitals in NH_3 molecules were included in the MRSDCI.

3. Optimized Structures and Energetics

The most stable structures of $Na_2^-(NH_3)_n$ ($n \leq 6$) and their total binding energies are shown in Figure 2, while those of the less stable isomers are in the Supporting Information (Figure 1S). We describe the total binding energy with both ZP and CP ($\Delta E_{ZPC+CPC}$) corrections below, unless mentioned otherwise.

In the lowest-energy structures for $n \leq 2$, one of the Na atoms has as many Na−N bonds as possible. $\Delta E_{ZPC+CPC}$ values were 5.8 and 12.8 kcal/mol for **1a** and **2a**, respectively. The isomers

TABLE 1: Vertical Detachment Energies (eV) Corresponding to Transitions from Anionic State to Neutral Ground and Low-Lying Excited States of $Na_2(NH_3)_n$ ($n = 0-6$) by the MRSDCI Method

$n=0$	**0a**		$n=1$	**1a**		$n=2$	**2a**		$n=3$	**3a**		**3b**		**3c**	
expt	state	calcd	expt	state	calcd	expt	state	calcd	expt	state	calcd	state	calcd	state	calcd
0.55	$1^1\Sigma_g^+$	0.54	0.41	1^1A_1	0.25	0.47	1^1A	0.30	0.51	1^1A	0.33	1^1A	0.34	1^1A	0.56
1.38	$1^3\Sigma_u^+$	1.22	1.36	1^3A_1	1.21	1.39	1^3A	1.25	1.39	1^3A	1.23	1^3A	1.26	1^3A	1.20
	$1^3\Pi_u$	2.14	1.86	1^3E	1.63		1^3B	1.52		2^3A	1.42	1^3E	1.45	2^3A	1.52
							2^3B	1.57		3^3A	1.44			3^3A	1.60
2.32	$1^1\Sigma_u^+$	2.14	2.11	2^1A_1	1.92	1.90	2^1A	1.76	1.71	2^1A	1.58	2^1A	1.57	2^1A	1.44
	$1^3\Sigma_g^+$	2.57	2.40	2^3A_1	2.16	2.17	2^3A	1.89	2.07	4^3A	1.75	2^3A	1.71	4^3A	1.81
	$1^1\Pi_u$	2.97		1^1E	2.45		1^1B	2.17		3^1A	1.93	1^1E	1.94	3^1A	1.86
							2^1B	2.19		4^1A	1.93			4^1A	1.86
	$2^1\Sigma_g^+$	2.88		3^1A_1	2.53		3^1A	2.35		5^1A	2.25	3^1A	2.24	5^1A	2.19

$n=4$	**4a**		**4b**		$n=5$	**5a**		**5b**		$n=6$	**6a**		**6b**	
expt	state	calcd	state	calcd	expt	state	calcd	state	calcd	expt	state	calcd	state	calcd
0.48	$1^1A'$	0.43	1^1A	0.56	0.52	$1^1A'$	0.40	1^1A	0.32	0.50	1^1A	0.33	$1^1A'$	0.30
1.48	$1^3A'$	1.31	1^3A	1.23	1.53	$1^3A'$	1.30	1^3A	1.06	1.54	1^3A	1.28	$1^3A'$	1.24
	$2^3A'$	1.41	1^3B	1.49		$1^3A''$	1.38	1^3E	1.07		2^3A	1.31	$1^3A''$	1.30
	$1^3A''$	1.42	2^3B	1.52		$2^3A'$	1.43				3^3A	1.39	$2^3A'$	1.35
1.65	$2^1A'$	1.51	2^1A	1.39		$2^1A'$	1.51	2^1A	1.17		2^1A	1.55	$2^1A'$	1.48
2.07	$3^3A'$	1.77	2^3A	1.73	1.90	$3^3A'$	1.73	2^3A	1.39	1.89	4^3A	1.68	$3^3A'$	1.61
	$3^1A'$	1.83	1^1B	1.78	2.01	$3^1A'$	1.82	1^1E	1.47	2.00	3^1A	1.75	$1^1A''$	1.75
	$1^1A''$	1.83	2^1B	1.78		$1^1A''$	1.82				4^1A	1.79	$3^1A'$	1.76
	$4^1A'$	2.13	3^1A	2.10		$4^1A'$	2.11	3^1A	1.64		5^1A	2.06	$4^1A'$	2.00

for $n = 1$ where the NH_3 molecule is bound from the H side to Na_2^- were higher than **1a** by 3.7 kcal/mol. The $Na^-(H_3N)_2$-Na- and $(H_3N)Na_2^-(NH_3)$-type isomers were less stable than **2a** by ~1 and 4.6 kcal/mol, respectively. The electronic distribution of the clusters will be described in detail later. The other isomers with fewer Na−N bonds were more unstable, and $\Delta E_{ZPC+CPC}$ of the $Na^-(H_3N)Na(NH_3)$-type complex was only 1.4 kcal/mol.

On the basis of the relative energies of 15 $n \leq 2$ isomers, the structures where one of the Na atoms has at least $(n - 1)$ Na−N bonds were optimized for $n \geq 3$. It was found that the first shell of the single Na in $Na_2^-(NH_3)_n$ completes at $n \simeq 4$, being similar to the neutral $Na(NH_3)_n$.[8] **3a**−**c** were almost isoenergetic, having $\Delta E_{ZPC+CPC}$ 19.2−19.0 kcal/mol. The Na−Na bonds are slightly elongated from that of free Na_2^- in **3a** and **b**, while it is longer than 5.4 Å in **3c**. The other $Na^-(H_3N)_3Na$-type isomer was less stable than **3a**−**c** by ~1 kcal/mol. The structures in which the single Na has at most two Na−N bonds were high-energy isomers. For $n = 4$, the $Na^-(H_3N)_3Na(NH_3)$- and $Na^-(H_3N)_2Na(NH_3)_2$-type clusters, **4a** and **4b**, were the most stable, and their $\Delta E_{ZPC+CPC}$ values were 27.5 and 26.9 kcal/mol, respectively. The other $Na^-(H_3N)_3Na(NH_3)$-type cluster and the isomers having $Na(NH_3)_3$-type partial structures were less stable than **4a** by more than 2 kcal/mol.

For $n = 5$ and 6, not only the clusters with the second shells but also the complexes between $Na(NH_3)_{n-1}$ and Na^-NH_3 were the low-energy isomers, in addition to the $Na^-(H_3N)_nNa$ -type structures. The most stable structure for $n = 5$ is **5a**, in which the fifth NH_3 molecule in the second shell of $Na(NH_3)_5$ is bound to the bare Na^-. Its $\Delta E_{ZPC+CPC}$ was 30.6 kcal/mol. The $(H_3N)Na^-(H_3N)_3Na(NH_3)$-type structure was less stable than **5a** by 0.6 kcal/mol. Two isomers were found where $Na(NH_3)_5$ with all solvents in the first shell was bound to Na^-, but they were higher than **5a** by 1.6−2.0 kcal/mol. Similarly, in the low-energy complexes for $n = 6$, the $Na(NH_3)_5(NH_3)_1$-, $Na(NH_3)_4(NH_3)_2$-, and $Na(NH_3)_6$-type partial structures are bound to Na^-, though only the most stable structures **6a** and **b** are shown in Figure 2. In addition, the complex consisting of $Na(NH_3)_5$ and Na^-NH_3 was stable. The $\Delta E_{ZPC+CPC}$ of those four structures ranged from 34.6 to 33.7 kcal/mol.

4. Vertical Detachment Energies and Analysis of Photoelectron Spectra

4.1. Summary of Experimental Spectra. The peak positions of the observed PES bands are indicated by color bars in Figure 1a to show their size dependence clearly. Three bands are observed at 0.55, 1.38, and 2.32 eV for Na_2^-, which is almost the same as the spectrum reported by Bowen's group.[61] The first broad band is shifted to ~0.4 eV from $n = 0$ to $n = 1$ and is gradually shifted back to ~0.5 eV at $n = 6-8$ with increasing n. The second broad band is located at 1.36, 1.39, and 1.39 eV for $n = 1-3$, respectively, and is slowly blue-shifted by further solvation to ~1.6 eV at $n = 8$.[49,50] There is a shoulder band at 1.86 eV and two strong bands at 2.11 and 2.40 eV for $n = 1$, while two distinct bands are found at 1.90 and 2.17 eV for $n = 2$ and at 1.71 and 2.07 eV for $n = 3$. Those bands are rapidly red-shifted narrowing the separation as n increases and are almost superimposed on the second broad band for $n \geq 4$. Shoulder peaks are observed at 1.65 and 2.07 eV for $n = 4$, at 1.90 and 2.01 eV for $n = 5$, and at 1.89 and 2.00 eV for $n = 6$.

4.2. Free Na_2^-. The calculated vertical detachment energies (VDEs) for the low-energy structures of $Na_2^-(NH_3)_n$ ($n = 0-6$) are listed in Table 1 together with the EBEs of the observed bands,[49,50] while those for the high-energy isomers are in the Supporting Information (Table 1S). The present VDEs for the bare Na_2^- agree almost perfectly with those by the CI calculations reported by Bonačić-Koutecký et al.[62,63] The observed bands were assigned to the transitions from the anionic state to the ground and low-lying excited states of the neutral, $1^1\Sigma_g^+$, $1^3\Sigma_u^+$, $1^3\Pi_u^+$, and $1^1\Sigma_u^+$ states. The last two states were accidentally degenerate at the anionic geometry. The VDE for the transition to the $1^1\Sigma_g^+$ was 0.54 eV in excellent agreement with the EBE for the first band, while those to the $1^3\Sigma_u^+$ and the higher degenerate states were 1.22 and 2.14 eV, respectively, which deviated from the corresponding EBEs by at most 0.2 eV. The transitions to the $1^3\Sigma_g^+$, $2^1\Sigma_g^+$, and $1^1\Pi_u$ states were predicted at 2.57−2.97 eV by the calculations, though no clear bands are observed in the energy region above 2.5 eV. The disagreement may be due to the low electron collection efficiency in the energy range near the detachment energy.

4.3. $Na_2^-(NH_3)_{1-3}$. The $n = 1$ and 2 spectra have been assigned by examining the VDEs of many isomers by the MRSDCI method at the CASSCF-optimized geometries and have been attributed to **1a** and **2a**, respectively.[49] The spectrum for $n = 3$ has been ascribed to the structure in which a single Na has three Na−N bonds on the basis of the relative energies of **3b**, **3e**, and **3g**-like forms optimized at the restricted open-shell Hartree−Fock level.[49] The present VDEs coincided with the corresponding literature values within ∼0.1 eV for $n = 0-2$. **3b** was also one of the most stable structures for $n = 3$ by the present MP2 calculations.

The VDEs for the most stable structures for each $n = 0-6$ are illustrated in Figure 1b. Though the calculations tend to underestimate the absolute EBEs of the observed bands by at most ∼0.3 eV, their shifts against n are reproduced remarkably well.

The first bands at ∼0.4 eV for both $n = 1$ and 2 were ascribed to the transition to the $1^1\Sigma_g^+$-type state in **1a** and **2a**, respectively. The VDEs for this transition decreased from Na_2^- to **1a** but increased slightly from **1a** to **2a** in agreement with the band shifts. The bands derived from the low-energy complexes such as **3a**−**c** are expected to overlap in the $n = 3$ spectrum. Because of the close VDEs and broadness of the observed bands, it is difficult to definitely distinguish their transitions in the spectrum. Nevertheless, the VDEs for the $1^1\Sigma_g^+$-type transition in **3a**−**c** increased slightly from that in **2a**, in accordance with the observation. The second bands at ∼1.4 eV for $n = 1-3$ were assigned to the $1^3\Sigma_u^+$-type transition in **1a**, **2a**, and **3a**−**c**. Their VDEs were ∼1.2 eV being consistent with the observed near constancy of the peak positions for $n = 0-3$. The shoulder at 1.86 eV for $n = 1$ was ascribed to the $1^3\Pi_u$-type transition in **1a**. The decrease of the VDE from Na_2^- to **1a** (0.51 eV) coincided well with the band shift (−0.46 eV) from $n = 0$ to $n = 1$. The VDEs for the transitions to the $1^3\Pi_u$-type states in **2a**, 1^3B, and 2^3B were 1.52 and 1.57 eV, respectively, decreasing further from that of **1a** by ∼0.1 eV. The corresponding bands are not sufficiently resolved to be identified in the spectra for $n = 2$, but it is most likely that they are superimposed on the strong $1^3\Sigma_u^+$-type band at ∼1.4 eV. The VDEs to the $1^3\Pi_u$-type state in **3a**−**b** were 1.42−1.45 eV, while that to the $1^1\Sigma_u^+$-type state in **3c** was 1.44 eV. They were further lowered from the VDE for the $1^3\Pi_u$-type transition in **2a**, indicative of the coalescence of corresponding bands on the intense 1.39-eV band in the $n = 3$ spectrum. The $1^1\Sigma_u^+$-type transition in **1a**, **2a**, and **3a**−**b** is considered to be responsible for the 2.11-, 1.90-, and 1.71-eV bands for $n = 1-3$. The VDEs for this transition decreased in a stepwise fashion by ∼0.2 eV from Na_2^- to **3a**−**b**, agreeing with the observed band shifts for $n = 0-3$. The $1^3\Pi_u$-type transition in **3c**, whose VDE was as large as those for the $1^1\Sigma_u^+$-type transition in **3a**−**b**, probably overlaps on the 1.71-eV band for $n = 3$. The VDEs to the $1^3\Sigma_g^+$- and $1^1\Pi_u$-type states in **1a** were 2.16 and 2.45 eV, respectively. Taking into account the underestimation of the EBEs by the calculations, the transition to the $1^3\Sigma_g^+$-type state is the more plausible candidate than that to the $1^1\Pi_u$- type state for the 2.40-eV band for $n = 1$. By a similar argument, the 2.17-eV band for $n = 2$ was assigned to the $1^3\Sigma_g^+$-type transition in **2a**, while the 2.07-eV band for $n = 3$ was assigned to the same transition in **3a**−**c**. The decrease of the VDEs for this transition was 0.27 eV from **1a** to **2a** and was 0.08−0.18 eV from **2a** to **3a**−**c**, in agreement with the observed lowering of the EBEs, 0.23 eV from $n = 1$ to $n = 2$, and 0.10 eV from $n = 2$ to $n = 3$, respectively.

4.4. $Na_2^-(NH_3)_{4-6}$. There is no discernible change except the spectral shifts between $n = 3$ and 4 in the PES, though the $n \geq 4$ clusters tend to have the Na^--$(H_3N)_n$Na form with long Na−Na separation. However, it is natural to expect that the most stable structures should contribute to the observed spectra for $n = 4-6$. In addition, it is likely that the transitions in the close-energy isomers such as **4b**, **5b**, and **6b** overlap. Although we cannot definitely assign the broad spectra for these sizes, the VDEs for the transitions to the ground and low-lying excited states in **4a**−**6a** match the EBEs of the peak positions as seen in Figure 1. The VDEs to the $1^1\Sigma_g^+$-type state were 0.43−0.33 eV in **4a**−**6a**, which were reasonably near the EBEs of the first bands at ∼0.5 eV for $n = 4-6$, while those for the $1^3\Sigma_u^+$-type transitions were 1.31−1.28 eV, being close to the EBEs of the second bands, ∼1.5 eV. The $1^3\Sigma_u^+$-type states were above the neutral ground state by ∼0.9 eV in all of these $n = 4-6$ clusters, in agreement with the roughly constant separation between the first and second bands.

The VDEs to the $1^3\Pi_u$-type states were ∼1.4 eV in **4a**−**6a**, which were as large as those in **3a**−**b**. This transition probably overlaps with the second band and is unresolved in the $n \geq 4$ spectra as in the case of $n = 3$. The VDEs to the $1^1\Sigma_u^+$-type state were 1.51−1.55 eV in **4a**−**6a**, which were near those in **3a**−**b**. The $1^1\Sigma_u^+$- and $1^3\Sigma_g^+$-type transitions in **4a** seem accountable for the shoulder peaks at 1.65 and 2.07 eV for $n = 4$, though the $1^1\Pi_u$-type transition may overlap the $1^3\Sigma_g^+$-type one. The $1^1\Sigma_u^+$-type band is considered to be unresolved for $n = 5$ and 6. The shoulders at 1.90 eV for $n = 5$ and at 1.89 eV for $n = 6$ are in a higher EBE region than the $1^1\Sigma_u^+$-type band for $n = 4$. Thus, the $1^3\Sigma_g^+$-type transition in **5a** and **6a**, whose VDEs were 1.73 and 1.68 eV, respectively, is the more probable candidate for those shoulders than the $1^1\Sigma_u^+$-type transition. The other shoulders at 2.01 eV for $n = 5$ and at 2.00 eV for $n = 6$ probably stem from further high states such as $1^1\Pi_u$-type states in **5a** and **6a**.

Takasu et al. have recorded the PESs for $n = 0-3$ and those for 3−5 using the low detachment energies.[50] The assignment of the PES by the better resolution is discussed in the Supporting Information (Appendix 1).

5. Electronic States

5.1. Anionic State. The natural orbitals (NOs) of the CI wave functions were calculated for $Na_2^-(NH_3)_n$. The occupation numbers of the NOs derived from the $4\sigma_g$ and $4\sigma_u$ orbitals of Na_2^- were ∼1.8 and ∼1.0, respectively, for all n. Those NOs are designated doubly occupied molecular orbital (DOMO) and singly occupied molecular orbital (SOMO), respectively, as shown below. The integrated electron densities of DOMO and SOMO, $\rho_i(z)$, as a function of z were evaluated using the following formula, where n_i^{occ} is the occupation numbers of each NO.

$$\rho_i(z) = \int_{-\infty}^{+\infty}\int_{-\infty}^{+\infty} n_i^{occ}\phi_i^2(x, y, z)\mathrm{d}x\mathrm{d}y \quad (i = \text{DOMO or SOMO}) \quad (2)$$

The z-axis was set to a line passing through two Na atoms with the midpoint of Na−Na at the origin. The free Na atom is in the negative z direction. The results are shown in Figure 3. The Na atoms in Na_2^- are located at ±1.836 Å, while those in **1a** are at ±1.714 Å. In the larger clusters, they are at ±1.767 Å (**2a**) to ±2.778 Å (**5a**). The peak positions of $\rho_{DOMO}(z)$ are shifted gradually from the origin to the negative z side as n increases and are finally located near the free Na for $n = 4-6$. On the other hand, the left peaks of $\rho_{SOMO}(z)$ are suddenly lowered from $n = 0$ to $n = 1$ and become almost invisible in the negative z region for $n > 1$, while the peaks in the positive

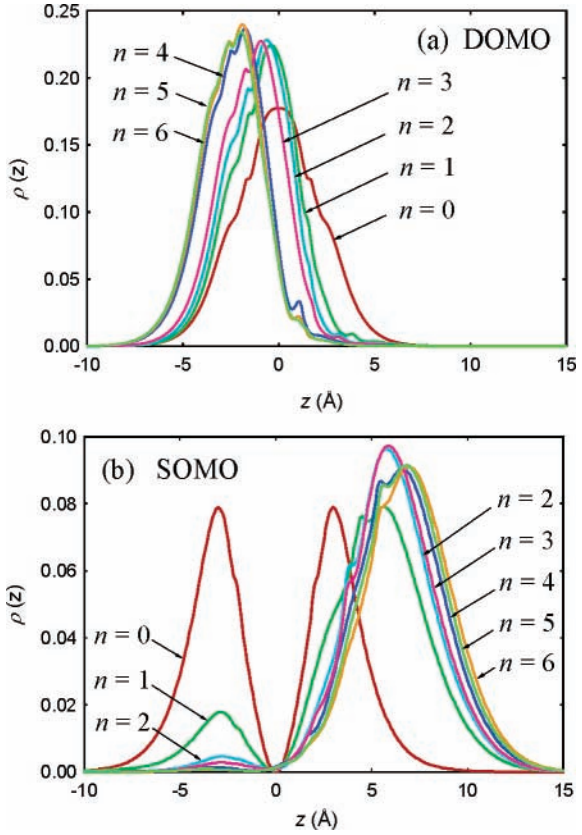

Figure 3. The integrated electron densities of DOMO and SOMO for the most stable structures of $Na_2^-(NH_3)_n$ ($n = 0-6$) as a function of z evaluated by eq 2.

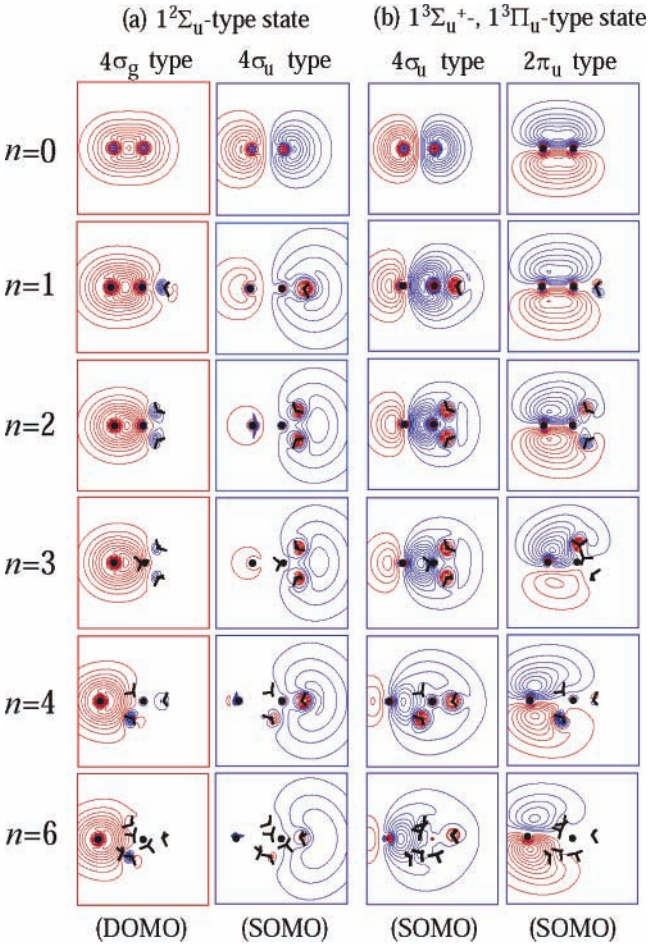

Figure 4. Contour maps of (a) DOMO and SOMO for Na_2^-, **1a**, **2a**, **3a**, **4a**, and **6a**, and (b) higher SOMOs of $1^3\Sigma_u^+$- and $1^3\Pi_u$-type states of their neutrals. The spacing of the contours is 0.005 Bohr$^{-3/2}$. The solvated Na is at the center, and the side length of each rectangle is 16 Å.

z side are shifted to the right with increasing n and are slightly high in **2a**−**6a** compared to Na_2^-. These observations indicate the developing Na^-−$Na(NH_3)_n$-type character, which is consistent with the EBEs of $Na^-(NH_3)_n$ and Na^-. The EBEs of $Na^-(NH_3)_n$ are a little lower than that of Na^-.[8] In addition, the width of $\rho_{SOMO}(z)$ increases with increasing n and its peaks are located outside the outermost hydrogen atoms at 4.255−5.707 Å in **1a**−**6a**. The number of electrons distributed in space on the right-hand side of the outermost hydrogen was 0.59 for **1a** but had become ∼0.8 for **2a**.

The contour maps of those NOs in the most stable forms for $n = 0-4$ and 6 are shown in Figure 4. With increasing n, the DOMO becomes localized near the free Na, while the SOMO is spatially expanded around the solvated Na in harmony with Figure 3. Both Figures 3 and 4 show the spontaneous ionization of the solvated Na and thus the growing Na^-−$Na^+(NH_3)_n(e^-)$-type state. The diffused excess electron surrounding $Na^+(NH_3)_n$ is expected to be ejected by the photodetachment in the $n \geq 2$ clusters.

5.2. Neutral Ground State. The contour maps of the DOMO for the neutral ground state were almost the same as those for the corresponding anions and thus are not shown for brevity. The DOMO changes from the σ-type molecular orbital to the 3s-like atomic orbital on the free Na as the one-side solvation of Na_2^- proceeds. Taking into account the structure and electronic state together, the ground state of $Na_2(NH_3)_n$ with $n \geq 4$ can be regarded as the Na^-−$Na^+(NH_3)_n$ type ion-pair complexes at the geometries of the anions, though this state correlates to the neutral $Na(3^2S)$ and $Na(3^2S)$ $(NH_3)_n$ at the dissociation limit.

The Na−Na $(NH_3)_n$ clusters can be approximately viewed as a heteronuclear alkali dimer. It is known from the drop of the ionization energies that the 3s(Na) level in $Na(NH_3)_n$ is raised by the mixing of the lone pair orbitals in ligands. As a result, the 3s orbital in the bare Na should become the major component in the $4\sigma_g$-type orbital in $Na_2(NH_3)_n$, which is consistent with Figure 4a. The EBE of the first PES band decreases by ∼0.14 eV from $n = 0$ to $n = 1$ as mentioned, implying that the solvation energy of $Na_2^-(NH_3)$ is smaller than that of $Na_2(NH_3)$. In fact, the ΔE of **1a** with only CPC was less than that of the corresponding neutral by 4.0 kcal/mol (0.17 eV). One can see a shoulder of $\rho_{SOMO}(z)$ at around ∼2 Å for **1a**, making the line for $n = 1$ distinguishable from others in this z area in Figure 3. The Na−N bond in both the anionic and neutral states should be ionic. However, the excess electron distributed in the Na−N bond region is considered to play some role in reducing the binding energy of the anion compared to the neutral. The first band is blue-shifted by 0.04 eV from $n = 1$ to $n = 2$, and the EBEs of the bands increase with reduced variations for larger n. The ΔE values with CPC were less than those of the neutrals by 2.1(0.09), 1.4(0.06), −0.6(−0.03), −0.8(−0.04), and 1.5(0.07) kcal/mol(eV), for **2a**−**6a**, respectively. The deviations of ΔEs between the anionic and neutral states diminish for $n \geq 2$, because the most excess electron is squeezed out of the first shell in the anions and has little effect on the ionic Na^+−$(NH_3)_n$ bonds for these sizes.

5.3. $1^3\Sigma_u^+$-, $1^3\Pi_u$-Type State. As is known from the photoelectron spectra of $Na^-(NH_3)_n$ and the absorption spectra of $Na(NH_3)_n$, the $3^2P(Na)-3^2S(Na)$ separation is reduced by

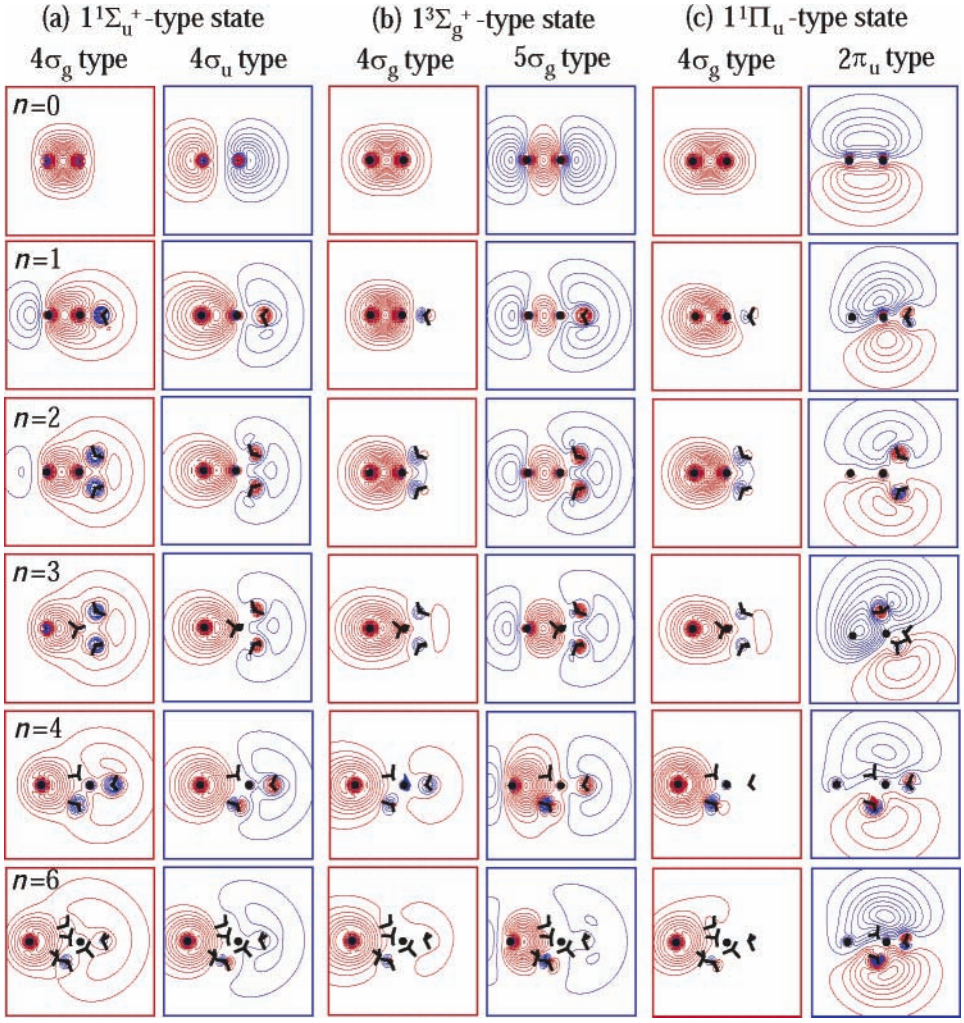

Figure 5. Contour maps of (a) $4\sigma_g$- and $4\sigma_u$-type NOs for the $1^1\Sigma_u^+$-type states and higher SOMOs of (b) $1^3\Sigma_g^+$- and (c) $1^1\Pi_u$-type states of neutrals at the geometries of Na_2^-, **1a**, **2a**, **3a**, **4a**, and **6a**, respectively. The spacing of the contours is 0.005 $Bohr^{-3/2}$. The solvated Na is at the center and the side length of each rectangle is 16 Å.

the addition of NH_3 molecules. As a result, the major components of low-lying vacant orbitals of Na−Na $(NH_3)_n$ are the 3p orbitals on the bare Na as well as the 3s and 3p orbitals on Na in the $Na(NH_3)_n$ parts.

An electron is promoted from the $4\sigma_g$-type orbital to the $4\sigma_u$- and $2\pi_u$-type orbitals in the $1^3\Sigma_u^+$- and $1^3\Pi_u$-type states, respectively. Since the $4\sigma_g$-type NOs for these states essentially resemble those in Figure 4a, only the contour maps of the other SOMOs are shown in Figure 4b. The $4\sigma_u$-type SOMO for the $1^3\Sigma_u^+$-type state is an antibonding orbital of 3s(Na) in Na_2, while it has the nature of a p-like orbital on the bare Na mixed with an s-like orbital in $Na(NH_3)_n$ for $n \geq 1$. The observed near-parallel shifts of the first and second bands can be attributed to the roughly constant separations between the $(3s)^2$ and $(3s)^1(3p)^1$ states in Na^- perturbed by the presence of $Na^+(NH_3)_n$. In the SOMOs for $n \geq 4$, the atomic 3p orbital is weakly mixed in comparison with the small sizes, but in turn the diffuse s-like character grows in the $Na(NH_3)_n$ side, which is a sign of the weak electron transfer from Na^- to $Na^+(NH_3)_n$, namely, the beginning of the radical-pair nature in $Na_2(NH_3)_{n\geq\sim4}$ complexes with long Na−Na separations. The lowest $^3\Sigma$-type state in the $n \geq \sim4$ clusters can be regarded as an intermediate state whose major configuration is slowly changing from the $(3s)^1(3p)^1$ of Na^- with $Na^+(NH_3)_n$ to the combination of the $(3s)^1$ of each Na, which is natural because this state correlates to the 3^2S-(Na)−3^2S(Na) asymptote. The electron transfer to the $Na(NH_3)_n$ part is expected to weaken the ionic character of the Na−N bonds in the $1^3\Sigma_u^+$-type state compared with the anionic state. Hence, the incremental solvation energies of this excited state should be less than those of the anions for $n \geq \sim4$, which well corresponds with the commencement of the blue shifts of the second band at $n = 4$.

On the other hand, the 3p(Na) orbital on Na^- becomes increasingly dominant in the $2\pi_u$-type SOMO for $n \geq 1$. The nature of the atomic 3p(Na)−3s(Na)-type transition in both the $1^3\Sigma_u^+$- and $1^3\Pi_u$-type states is considered to be responsible for the observed coalescence of the shoulder on the second band at $n \geq 2$.

5.4. $1^1\Sigma_u^+$-, $1^3\Sigma_g^+$-, and $1^1\Pi_u$-Type States. The contour maps of the SOMOs for the $1^1\Sigma_u^+$-, $1^3\Sigma_g^+$-, and $1^1\Pi_u$-type states are illustrated in Figure 5. The SOMOs for the $1^1\Sigma_u^+$-type state are distributed in both Na and $Na(NH_3)_n$ sides and are of covalent nature rather than ionic. The lower SOMO is the in-phase mixture of the 3p(Na) and the diffuse 3s(Na) orbital in $Na(NH_3)_n$, while the higher one is the in-phase combination of the 3s(Na) and the diffuse 3p(Na) for $n = 1$ and 2. These SOMOs become the bonding and antibonding orbitals of the 3s(Na) and the diffuse 3s(Na), respectively, for $n \geq \sim3$, clearly indicating the radical-pair character. Two unpaired electrons separate from each other as Na and $Na(NH_3)_n$ become distant. As a result, the singlet−triplet splitting between the $1^1\Sigma_u^+$-type state and its triplet counterpart $1^3\Sigma_u^+$-type state diminishes,

which is considered responsible for the near degeneracy of the $1^3\Sigma_u^+$- and $1^1\Sigma_u^+$-type states for these sizes.

In both the $1^3\Sigma_g^+$- and $1^1\Pi_u$-type states, the lower SOMO changes from the $4\sigma_g$-like molecular orbital to the atomic 3s-(Na) orbital with increasing n. The other SOMO in the former state in Na_2 is a $5\sigma_g$-like orbital, and the 3p (Na) orbital of Na-$(NH_3)_n$ with increased diffuseness becomes a major contributor as n increases. Similarly, the diffuse 3p-π orbital of $Na(NH_3)_n$ is dominant in the second SOMO for the latter state for $n > 0$. Thus, these $1^3\Sigma_g^+$- and $1^1\Pi_u$-type states are also the radical-pair state correlating to the ground-state $Na(3^2S)$ and the excited $Na^*(3^2P)(NH_3)_n$. The convergence of the $1^3\Sigma_g^+$- and $1^1\Pi_u$-type bands toward the $1^1\Sigma_u^+$-type band results from the known reduction in the $^2S-{}^2P$ separations in $Na(NH_3)_n$ perturbed by the near Na.

6. Conclusions

In this study, we have calculated the geometries, total binding energies, and vertical detachment energies of $Na_2^-(NH_3)_n$ ($n \leq 6$) by ab initio MO methods and have studied the electronic nature of both anionic and neutral states in connection with the photoelectron spectra. The conclusions we have reached are as follows:

(1) The $Na^-{-}Na^+(NH_3)_n(e^-)$-type state is the most stable for the anions. The lowest-energy structures for each $n \geq 4$ can be regarded as the complex between Na^- and $Na(NH_3)_n$. The neutral ground state is also an ion pair having $Na^-{-}Na^+$-$(NH_3)_n$-type nature. The diffused solvated electron is expected to be ejected by the photodetachment in the $n \geq 2$ anion clusters.

(2) The Na−N bonds are ionic in both the anionic and neutral clusters. The binding energy of a single NH_3 is larger in the neutral complex than in the anion complex, which results in the red shift of the first band from $n = 0$ to $n = 1$. As the excess electron is expelled from the first shell by further solvation, the deviations of total binding energies between the anionic and neutral states decrease, which is reflected in the gradual blue shifts of the first PES bands.

(3) The lowest-lying excited states of the neutrals are derived from the $1^3\Sigma_u^+$ and $1^3\Pi_u$ states of Na_2. They are also ionic and show the character of Na^- perturbed by the presence of Na^+-$(NH_3)_n$, which is responsible for the near-parallel shifts of the first and second PES bands as well as the sudden coalescence of the shoulder band on the second band at $n \geq 2$. It is also found that the radical pair character slowly develops in the $1^3\Sigma$-type state for $n \geq \sim 4$.

(4) The $1^1\Sigma_u^+$-type state also becomes increasingly the radical-pair state consisting of $Na(3^2S)$ and $Na(3^2S)(NH_3)_n$. The narrowing of the separation between the $1^3\Sigma_u^+$- and the $1^1\Sigma_u^+$-type bands is considered to be due to the diminishing singlet−triplet splitting between those states in $Na-Na(NH_3)_{4-6}$ complexes with long Na−Na distances.

(5) The higher states derived from the $1^3\Sigma_g^+$ and $1^1\Pi_u$ of Na_2 are the $Na(3^2S)-Na^*(3^2P)(NH_3)_n$-type excited states. The red shifts of the $1^3\Sigma_g^+$- and $1^1\Pi_u$-type bands toward the $1^1\Sigma_u^+$-type band with increasing n can be attributed to the known reduction in the 3^2S-3^2P separation in $Na(NH_3)_n$.

Acknowledgment. This work was financially supported in part by a Grant-in-Aid from the Ministry of Education, Culture, Science, Sports, and Technology of Japan. We thank Dr. R. Okuda and Dr. N. Miura for their assistance in the early stages of this work. We are also grateful to Professor Fuke (Kobe University) for providing us the spectral data.

Supporting Information Available: Assignment of PES by low detachment energies (Appendix 1); optimized geometries and total binding energies of high-energy isomers (Figure 1S); vertical detachment energies of high-energy isomers (Table 1S). The information is available free of charge via the Internet at http://pub.acs.org.

References and Notes

(1) Fuke, K.; Hashimoto K.; Iwata S. In *Advances in Chemical Physics*; Prigogine, I, Rice, S. A., Eds.; Vol. 110; John Wiley & Sons: New York, 1999; Chapter 7, p 433.
(2) Fuke, K.; Hashimoto, K.; Takasu R. In *Advances in Metal and Semiconductor Clusters*; Duncan, M. A., Ed.; Vol. 5; Elsevier: New York, 2001; p 1.
(3) Schulz, C. P.; Haugstatter, R.; Tittes, H. U.; Hertel, I. V. *Phys. Rev. Lett.* **1986**, *57*, 1703.
(4) Hertel, I. V.; Huglin, C.; Nitsch, C.; Schulz, C. P. *Phys. Rev. Lett.* **1991**, *67*, 1767.
(5) Nitsch, C.; Schulz, C. P.; Gerber, A.; Zimmermann-Edling, W.; Hertel, I. V. *Z. Phys. D* **1992**, *22*, 651.
(6) Misaizu, F.; Tsukamoto, K.; Sanekata, M.; Fuke. K. *Chem. Phys. Lett.* **1992**, *188*, 241.
(7) Takasu, R.; Hashimoto, K.; Fuke, K. *Chem. Phys. Lett.* **1996**, *258*, 94.
(8) Takasu, R.; Misaizu, F.; Hashimoto, K.; Fuke, K. *J. Phys. Chem. A* **1997**, *101*, 3078.
(9) Takasu, R.; Taguchi, T.; Hashimoto, K.; Fuke, K. *Chem. Phys. Lett.* **1998**, *290*, 481.
(10) Shen, M. H.; Winniczek, J. W.; Farrar, J. M. *J. Phys. Chem.* **1987**, *91*, 6447.
(11) Shen, M. H.; Farrar, J. M. *J. Phys. Chem.* **1989**, *93*, 4386.
(12) Shen, M. H.; Farrar, J. M. *J. Chem. Phys.* **1991**, *94*, 3322.
(13) Donnelly, S. G.; Farrar, J. M. *J. Chem. Phys.* **1993**, *98*, 5450.
(14) Yeh, C. S.; Willey, K. F.; Robbins, D.; Pilgrim, J. S.; Duncan, M. A. *Chem. Phys. Lett.* **1992**, *196*, 233.
(15) Willey, K. F.; Yeh, C. S.; Robbins, D. L.; Pilgrim, J. S.; Duncan, M. A. *J. Chem. Phys.* **1992**, *97*, 8886.
(16) Scurlock, C. T.; Pullins, S. H.; Reddic, J. E.; Duncan, M. A. *J. Chem. Phys.* **1996**, *104*, 4591.
(17) Misaizu, F.; Sanekata, M.; Tsukamoto, K.; Fuke, K.; Iwata, S. *J. Phys. Chem.* **1992**, *96*, 8259.
(18) Fuke, K.; Misaizu, F.; Sanekata, M.; Tsukamoto, K.; Iwata, S. *Z. Phys. D* **1993**, *26*, 180.
(19) Misaizu, F.; Sanekata, M.; Fuke, K.; Iwata, S. *J. Chem. Phys.* **1994**, *100*, 1161.
(20) Yoshida, S.; Daigoku, K.; Okai, N.; Takahata, A.; Sabu, A.; Hashimoto, K.; Fuke, K. *J. Chem. Phys.* **2002**, *117*, 8657.
(21) Sanekata, M.; Misaizu, F.; Fuke, K. *J. Chem. Phys.* **1996**, *104*, 9768.
(22) Takasu, R.; Nishikawa, K.; Miura, N.; Sabu, A.; Hashimoto, K.; Schulz, C. P.; Hertel, I. V.; Fuke, K. *J. Phys. Chem. A* **2001**, *105*, 6602.
(23) Nitsch, C.; Huglin, C.; Hertel, I. V.; Schulz, C. P. *J. Chem. Phys.* **1994**, *101*, 6559.
(24) Schultz, C. P.; Nitsch, C. *J. Chem. Phys.* **1997**, *107*, 9794.
(25) Brockhaus, P.; Hertel, I. V.; Schulz, C. P. *J. Chem. Phys.* **1999**, *110*, 393.
(26) Schulz, C. P.; Bobbert, C.; Shimosato, T.; Daigoku, K.; Miura, N.; Hashimoto, K. *J. Chem. Phys.* **2003**, *119*, 11620.
(27) Marchi, M.; Sprik, M.; Klein, M. *Faraday Discuss., Chem. Soc.* **1988**, *85*, 373.
(28) Marchi, M.; Sprik, M.; Klein, M. *J. Phys.: Condens. Matter* **1990**, *2*, 5833.
(29) Martyna, G. L.; Klein, M. L. *J. Chem. Phys.* **1992**, *96*, 7662.
(30) Deng, Z.; Martyna, G. L.; Klein, M. L. *Phys. Rev. Lett.* **1993**, *71*, 267.
(31) Kohanoff, J.; Buda, F.; Parrinello, M.; Klein, M. L. *Phys. Rev. Lett.* **1994**, *73*, 3133.
(32) Stampfli, P.; Bennemann, K. H. *Comput. Mater. Sci.* **1994**, *2*, 578.
(33) Stampfli, P. *Phys. Rep.* **1995**, *255*, 1.
(34) Makov, G.; Nitzan, A. *J. Phys. Chem.* **1994**, *98*, 3549.
(35) Barnett, R. N.; Landman, U. *Phys. Rev. Lett.* **1993**, *70*, 1775.
(36) Hashimoto, K.; He, S.; Morokuma, K. *Chem. Phys. Lett.* **1993**, *206*, 297.
(37) Hashimoto, K.; Morokuma, K. *J. Am. Chem. Soc.* **1995**, *116*, 11436.
(38) Hashimoto, K.; Morokuma, K. *J. Am. Chem. Soc.* **1995**, *117*, 4151.
(39) Hashimoto, K.; Kamimoto, T. *J. Am. Chem. Soc.* **1998**, *120*, 3560.
(40) Ramania, M.; Bernasconi, M.; Parrinello, M. *J. Chem. Phys.* **1998**, *109*, 6839.
(41) Tsurusawa, T.; Iwata, S. *J. Phys. Chem. A* **1999**, *103*, 6134.
(42) Martyna, G. L.; Klein, M. L. *J. Phys. Chem.* **1991**, *95*, 515.

(43) Bauschlicher, C. W., Jr.; Sodupe, M.; Partridge, H. *J. Chem. Phys.* **1992**, *96*, 4453.
(44) Daigoku, K.; Hashimoto, K. *J. Chem. Phys.* **2004**, *121*, 3569.
(45) Hashimoto, K.; Kamimoto, T.; Fuke, K. *Chem. Phys. Lett.* **1997**, *266*, 7.
(46) Hashimoto, K.; Kamimoto, T.; Daigoku, K. *J. Phys. Chem. A* **2000**, *104*, 3299.
(47) Hashimoto, K.; Kamimoto, T.; Miura, N.; Okuda, R.; Daigoku, K. *J. Chem. Phys.* **2000**, *113*, 9540.
(48) Hashimoto, K.; Daigoku, K.; Kamimoto, T.; Shimosato, T. *Internet Electron. J. Mol. Des.* **2002**, *1*, 503; http://www.biochempress.com, ISSN: 1538-6414, CODEN: IEJMAT.
(49) Takasu, R.; Hashimoto, K.; Okuda, R.; Fuke, K. *J. Phys. Chem. A* **1999**, *103*, 349.
(50) Takasu, R.; Ito, H.; Nishikawa, K.; Hashimoto, K.; Okuda, R.; Fuke, K. *J. Electron Spectrosc. Relat. Phenom.* **2000**, *106*, 127.
(51) Frisch, M. J.; Trucks, G. W.; Schlegel, H. B.; Scuseria, G. E.; Robb, M. A.; Cheeseman, J. R.; Zakrzewski, V. G.; Montgomery, J. A., Jr.; Stratmann, R. E.; Burant, J. C.; Dapprich, S.; Millam, J. M.; Daniels, A. D.; Kudin, K. N.; Strain, M. C.; Farkas, O.; Tomasi, J.; Barone, V.; Cossi, M.; Cammi, R.; Mennucci, B.; Pomelli, C.; Adamo, C.; Clifford, S.; Ochterski, J.; Petersson, G. A.; Ayala, P. Y.; Cui, Q.; Morokuma, K.; Rega, N.; Salvador, P.; Dannenberg, J. J.; Malick, D. K.; Rabuck, A. D.; Raghavachari, K.; Foresman, J. B.; Cioslowski, J.; Ortiz, J. V.; Baboul, A. G.; Stefanov, B. B.; Liu, G.; Liashenko, A.; Piskorz, P.; Komaromi, I.; Gomperts, R.; Martin, R. L.; Fox, D. J.; Keith, T.; Al-Laham, M. A.; Peng, C. Y.; Nanayakkara, A.; Challacombe, M.; Gill, P. M. W.; Johnson, B.; Chen, W.; Wong, M. W.; Andres, J. L.; Gonzalez, C.; Head-Gordon, M.; Replogle, E. S.; Pople, J. A. *Gaussian 98*, revision A.11; Gaussian, Inc.: Pittsburgh, PA, 2001.
(52) Hertzberg, G. *Molecular Spectra and Molecular Structure II. Infrared and Raman Spectra of Polyatomic Molecules*; Van Nostrand Reinhold: New York, 1945.
(53) Boys, S. F.; Bernardi, F. *Mol. Phys.* **1970**, *19*, 553.
(54) Xantheas, S. S. *J. Chem. Phys.* **1996**, *104*, 8821.
(55) Werner, H. -J.; Knowles, P. J. *J. Chem. Phys.* **1985**, *82*, 5053.
(56) Knowles, P. J.; Werner, H. -J. *Chem. Phys. Lett.* **1985**, *115*, 259.
(57) Werener, H.-J.; Knowles, P. J. *J. Chem. Phys.* **1988**, *89*, 5803.
(58) Knowles, P. J.; Werner, H.-J. *Chem. Phys. Lett.* **1988**, *145*, 514.
(59) Knowles, P. J.; Werner, H. -J. *Theor. Chim. Acta* **1992**, *84*, 95.
(60) MOLPRO is a package of ab initio programs written by Werner, H. -J. and Knowles, P. J. with contributions from Amos, R. D.; Bernhardsson, A.; Berning, A.; Celani, P.; Cooper, D. L.; Deegan, M. J. O.; Dobbyn, A. J.; Eckert, F.; Hampel, C.; Hetzer, G.; Korona, T.; Lindh, R.; Lloyd, A. W.; McNicholas, S. J.; Mandy, F. R.; Meyer, W.; Mura, M. E.; Nicklass, A.; Palmieri, P.; Pitzer, R.; Rauhut, G.; Schütz, M.; Stoll, H.; Stone, A. J.; Tarroni, R.; Thorsteinsson, T.
(61) McHugh, K. M.; Eaton, J. G.; Lee, G. H.; Sarkas, H. W.; Kidder, L. H.; Snodgrass, J. T.; Manaa, M. R.; Bowen, K. H. *J. Chem. Phys.* **1989**, *91*, 3792.
(62) Bonačić-Koutecký, V.; Fantucci, P.; Koutecký, J. *J. Chem. Phys.* **1989**, *91*, 3794.
(63) Bonačić-Koutecký, V.; Fantucci, P.; Koutecký, J. *J. Chem. Phys.* **1990**, *93*, 3802.